Available online at www.eccomasproceedia.org
Eccomas Proceedia UNCECOMP (2023) 511-525

ECCOMAS
Proceedia

UNCECOMP 2023
5th ECCOMAS Thematic Conference on
Uncertainty Quantification in Computational Science and Engineering
M. Papadrakakis, V. Papadopoulos, G. Stefanou (eds.)
Athens, Greece, 12-14 June 2023

SENSITIVITY ANALYSIS FOR EFFECTIVE CONDUCTIVITY OF ANISOTROPIC FIBROUS MATERIALS

Kunkun Tang[1], Francesco Panerai[2], and Jonathan B. Freund[2]

[1]The National Center for Supercomputing Applications (NCSA)
University of Illinois Urbana-Champaign, Urbana IL 61801, USA
e-mail: ktg@illinois.edu

[2] Aerospace Engineering
University of Illinois Urbana-Champaign, Urbana IL 61801, USA
e-mail: {fpanerai,jbfreund}@illinois.edu

Abstract. *Due to production imperfection, substantial spatial variability is present in carbon-based composite materials. Moreover, there exists a high contrast of thermal properties between fibers and the void phase. This paper answers the question of how the effective thermal properties of the macroscale composite material change with respect to the geometric variability and to the conductivity discontinuity at the interfaces between fibers and air. The Porous Microstructure Analysis (PuMA) software is used in this work to artificially generate 3D random carbon fibers. Geometric variability is characterized by uncertian parameters ranging from fiber dimensions to orientations. This uncertainty model is then solved using Global Sensitivity Analysis method. We have found that the porosity of the material has the most significant influence on the effective property.*

Keywords: Thermal Conductivity, Anisotropic Materials, Carbon fiber, Porous Media, Global Sensitivity Analysis, ANOVA

ISSN:2623-3339
Peer-review under responsibility of the organizing committee of UNCECOMP 2023.
doi: 10.7712/120223.10354.19852

1 Introduction

It is known that composite materials are subject to substantial geometric variability due to manufacturing process [1], e.g, fiber size and length, fiber orientation, and porosity. It is thus beneficial to understand how this spatial variability affect the effective material properties in the macroscopic scale, for instance the effective thermal conductivity, which is of fundamental importance for the process of material resistance and degradation. A better understanding of this uncertainty model also helps design more accurate microstructures that translate into more precise estimation of the material response. In this paper, we are interested in the overall sensitivity, which is quantified with Global Sensitivity Analysis using the metric of Sobol' Total Sensitivity Indices to measure the relative importance of uncertain parameters that characterize the spatial variability in modeling a representative elementary volume of a composite carbon fiber material. In particular, we use the Porous Microstructure Analysis (PuMA) software [2] that has been developed at the NASA Ames Research Center to calculate material properties and response on large digital microstructures. PuMA has capabilities of importing microstructures originating from the microtomographic scans. However, we are only focused on the software's functionality of the artificial material generator which allows for the creation of random 3D fiber structures, packed sphere beds, periodic foam structures, and so on. More specifically, we are focused on the case of 3D random fibers in this paper.

2 Uncertainties in composite materials with isotropic components

The overall goal of this work is to assess uncertainty for a type of fiber-based composite material microstructures, and to understand how uncertainty in fiber packing and other properties impact predictions for their collective properties.

2.1 Estimation of effective conductivity for a composite material

We follow the method developed by Wiegmann and Zemitis [3] to compute the effective thermal conductivity of composite materials using a fast explicit jump harmonic averaging solver. This method is highly efficient based on 3D images (either from imaging devices or artificially generated) without the need of any further processing. The material as it enters the simulation is described by a rectangular parallelepiped of voxels. The numerics are performed on an equidistant Cartesian grid with temperature variables at the voxel centers. On each voxel the thermal conductivity is assumed constant. This method requires that the individual materials are isotropic. Two neighboring voxels corresponding to different materials lead to a jump across the interface for the coefficient in the heat equation. We summarize the main idea of the method in this section. Readers are refereed to the work by Wiegmann and Zemitis [3] for a thorough insight of the approach.

The classical heat equation is used to describe the heat transfer in materials due to diffusion,

$$\nabla \cdot (k \nabla T) = f \text{ in } \Omega, \tag{1}$$

with T the temperature, $k(\vec{x})$ the local conductivity at $\vec{x} = (x_1, x_2, x_3)$, $\Omega = (0, d_1) \times (0, d_2) \times (0, d_3)$ the rectangular parallelepiped, and f the heat source.

With the assumption of isotropic component materials, $k(\vec{x})$ is a scalar quantity. A composite material is generally anisotropic because of geometric anisotropy, whose effective thermal conductivity can be described as a tensor k^*. In order to determine this tensor k^* by using homogenization theory, it is first necessary to solve 3 different **singular**

periodic boundary value problems ($l = 1, 2, 3$) in Ω:

$$\begin{aligned} \nabla \cdot (k(\vec{x})(\nabla T_l + \vec{e}_l)) &= 0, \quad \vec{x} \in \Omega, \\ T_l(\vec{x} + id_1\vec{e}_1 + jd_2\vec{e}_2 + kd_3\vec{e}_3) &= T_l(\vec{x}), \quad i, j, k \in \mathbf{Z} \end{aligned} \tag{2}$$

where $\vec{e}_l$ is a unit vector in the direction x_l. After finding T_1, T_2, T_3, the component of the conductivity tensor can be obtained by computing the following integral

$$k^*_{ml} = \frac{1}{d_1 d_2 d_3} \int_\Omega < \vec{e}_m, k(\vec{x})(\nabla T_l + \vec{e}_l) > \, \mathrm{d}\vec{x}, \quad m, l = 1, 2, 3, \tag{3}$$

where $< \cdot, \cdot >$ denotes the inner product.

As explained by Wiegmann and Zemitis [3], the main difficulty in solving the system (2) is from the fact that the heat flux $k\nabla T_l$ has a jump in the direction $\vec{e}_l$ proportional to the difference in conductivities, which leads to the following jump condition,

$$\begin{aligned} [T_l]\,|_{\vec{x}=\vec{x}^*} &= 0, \\ \left[k\frac{\partial T_l}{\partial x_i}\right]|_{\vec{x}=\vec{x}^*} &= -\delta_{il}\,[k]\,|_{\vec{x}=\vec{x}^*} \quad \text{for } i = 1, 2, 3, \end{aligned} \tag{4}$$

where δ_{il} is Kronecker symbol and $[\cdot]$ is the jump across the interface $\vec{x} = \vec{x}^*$.

Wiegmann and Zemitis [3] presented the standard discretization method using harmonic averaging to solve (2) with (4), as well as a newly proposed approach by eliminating the solution variables, and keeping only the jump variables. As explained by the authors, their new approach formulated in terms of the discontinuities of the normal derivative across the interfaces has the advantage of being amenable to using two important and efficient numerical methods: a conjugate gradient variant for iteratively solving the Schur-complement, and the Fast Fourier Transformation for inverting the Laplacian in evaluating the Schur-complement matrix. Results show that very few iterations are needed to solve the Schur-complement even in the presence of large contrast in the local conductivity coefficients. Readers are refereed to [3] for details of the method. After the system (2) is solved, one can readily approximate the tensor of the effective thermal conductivity (3).

2.2 Parameters and their uncertainties

Let us introduce the uncertain parameters in our simulation model. The parameters needed to construct a sample microstructure are reported in Table 1 together with their nominal values and uncertain ranges. Most of the parameters in Table 1 are straightforward for their meanings, for example the fiber diameter d_{fiber} and length l_{fiber} with their variations, Δd_{fiber} and Δl_{fiber} respectively. The orientation angle parameter θ_l in direction x_l can vary from 0° to 90°, with 0° meaning that the fibers are perfectly aligned within the plane normal to x_l, and 90° meaning that the fibers are randomly oriented without any particular preferred direction. The volume fraction ψ_i of a given phase i is determined as a ratio of the number of voxels, N_i, in the phase to the total number of voxels, N_{tot}, in the domain: $\psi i = N_i/N_{\text{tot}}$. The porosity, ϕ, is defined as the volume fraction of the void phase. k_f and k_{air} are the local thermal conductivities of fiber and air, respectively. The local isotropy has been assumed for this paper.

Please note the above introduced parameters are necessary inputs in the PuMA software [2] to use its artificial material generator for the creation of random 3D fiber structures, in particular simple cylinders in this paper. Although PuMA has capabilities of

	Symbol	Value	Uncertainty/Status	Description
Material topology	d_{fiber}	$10\,\mu$m	$\mathcal{U}(8, 12)$	Fiber diameter
	Δd_{fiber}	$2\,\mu$m	$\mathcal{U}(0, 2)$	Fiber diameter variation
	l_{fiber}	1 mm	$\mathcal{U}(0.5, 1)$	Fiber length
	Δl_{fiber}	0.3 mm	$\mathcal{U}(0, 0.3)$	Fiber length variation
	θ_x	45°	$\mathcal{U}(0, 90)$	Orientation wrt x-normal plane
	θ_y	45°	$\mathcal{U}(0, 90)$	Orientation wrt y-normal plane
	θ_z	20°	$\mathcal{U}(0, 40)$	Orientation wrt z-normal plane
	ϕ	0.89	$\mathcal{U}(0.5, 0.95)$	Porosity
Thermal properties	k_f	$12\,\text{W}/(\text{m}\cdot\text{K})$	$\mathcal{U}(5, 100)$	Fiber conductivity
	k_{air}	$0.0257\,\text{W}/(\text{m}\cdot\text{K})$	$\mathcal{U}(0.008, 0.04)$	Air conductivity

Table 1: Parameters, their nominal values and associated uncertainties for models of microstructures generated from PuMA with random cylinders with local anisotropy.

importing as a 3D TIFF from micro-tomography, we only consider artificial microstructures in this work.

The geometric uncertainties reported in Table 1 are originated from the heterogeneous nature of the composite materials, i.e., the porosity, fiber size, and orientation are subject to substantial variability because of manufacturing process [1]. A uniform distribution has been assigned for all parameters due to unavailability of experimental data and lack of knowledge. In order to visually illustrate the meanings of geometric uncertain parameters, Figure 1a shows the microstructure artificially generated by PuMA using nominal values of these parameters, together with varied representations (Figures 1b–1j) by modifying a single parameter. In particular, we observe the variation of porosity ($\phi \in [0.5, 0.95]$) leads to considerably different material structures, and we thus anticipate the uncertainty of ϕ has significant impact on effective properties.

3 Variance decomposition and sensitivity analysis method

In this section, we introduce the established mathematical representation of the relation between input uncertain parameters and the effective thermal conductivity as the Quantity of Interest (QoI). In particular, an output variance decomposition is introduced and global sensitivity indices are then defined. This functional decomposition will lead to the understanding of how uncertain our QoI is and how this output uncertainty can be attributed to input uncertainties.

The basic representation we use is the functional decomposition of the model output f depending on an $\mathbb{R}^N$-valued input random vector $\vec{x} = \{x_1, \ldots, x_N\}$,

$$f(\vec{x}) = \sum_{u \subseteq \{1,\ldots,N\}} f_u(\vec{x}_u). \tag{5}$$

Here $f_u(\vec{x}_u)$ is called a $|u|$-th order component function of f, describing a constant or a $|u|$-variate interaction of $\vec{x}_u = \{x_{i_1}, \ldots, x_{i_{|u|}}\}$ on f when $|u|$ is zero or positive, respectively.

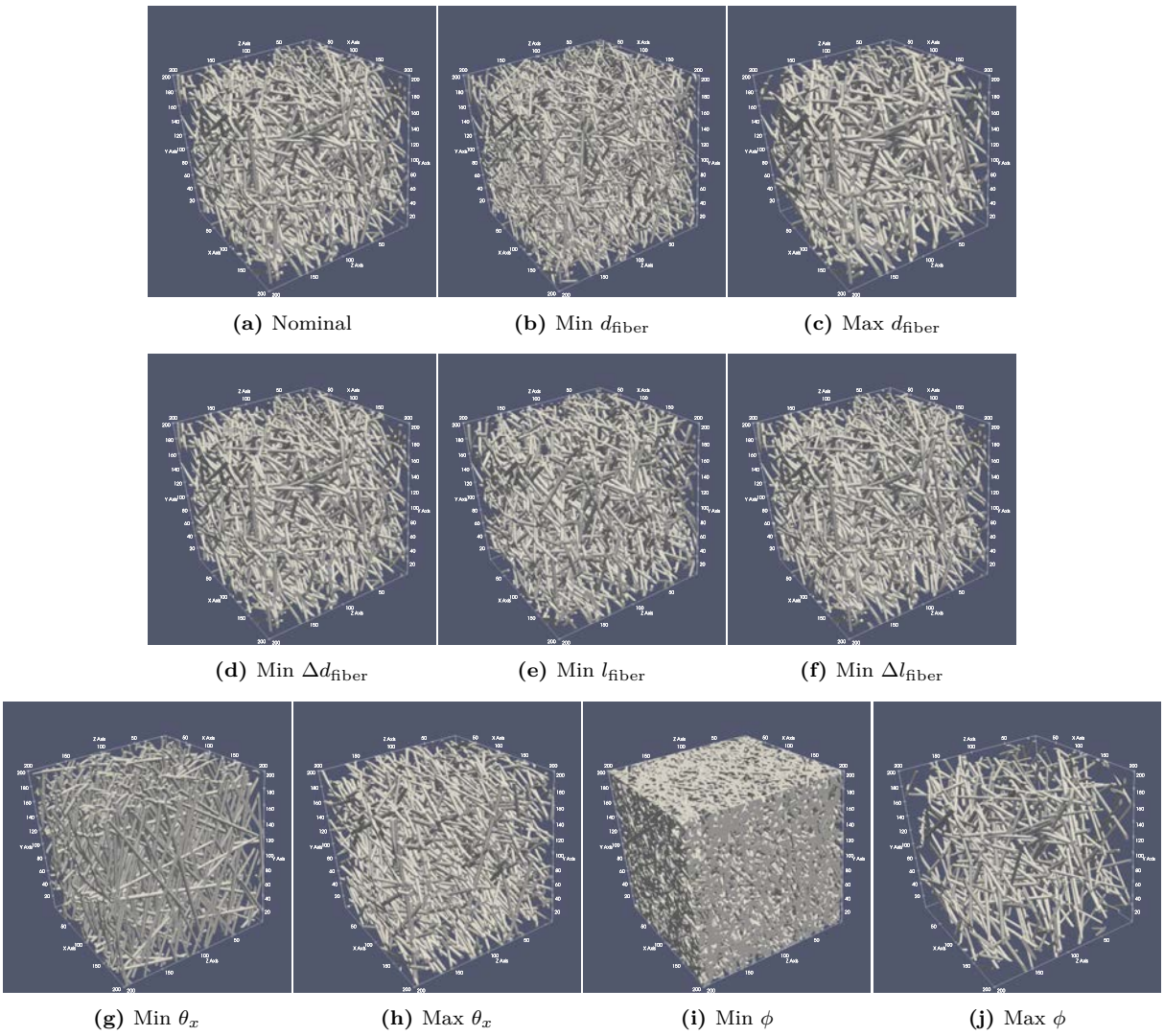

(a) Nominal **(b)** Min d_{fiber} **(c)** Max d_{fiber}

(d) Min Δd_{fiber} **(e)** Min l_{fiber} **(f)** Min Δl_{fiber}

(g) Min θ_x **(h)** Max θ_x **(i)** Min ϕ **(j)** Max ϕ

Figure 1: (a) An artificial microstructure representation of random cylinder fibers generated using PuMA with nominal values reported in Table 1; (b–j) Microstructures by varying only one parameter to its extreme value.

Thus an Analysis of Variance (ANOVA) expansion decomposes the original N-dimensional space into a union of subspaces, with each subspace representing a particular order of interaction among input parameters. Many problems only have low-order interactions and so are amenable to such a representation, making an ANOVA expansion useful despite the nominally poor asymptotic scaling of the number of terms required in the complete ANOVA expansion:

$$P_{\text{ANOVA}} = 2^N. \tag{6}$$

In this paper, we only consider an $\vec{x}$ whose members are *independent random variables* (Parameters introduced in Table 1 are uniformly distributed independent random variables). Thus the decomposition (5) is unique under the condition

$$\int_{\mathbb{R}} f_u(\vec{x}_u)\,\mathrm{d}F_i(x_i) = 0, \forall i \in u, \tag{7}$$

where $F_i(x_i)$ is the cumulative distribution function of x_i. Furthermore, component functions in (5) are orthogonal, resulting in that the *total variance* $V = \int_{\mathbb{R}^N}[f - E(f)]^2\,\mathrm{d}F(\vec{x})$

of output $f(\vec{x})$ is the summation of all *partial variances*

$$V = \sum_{\emptyset \neq u \subseteq \{1,\ldots,N\}} \mathrm{Var}(f_u). \tag{8}$$

$F(\vec{x})$ above is the joint cumulative distribution function of $\vec{x}$, and due to independence assumption the probability measure is a product $\mathrm{d}F(\vec{x}) = \prod_{i=1}^{N} \mathrm{d}F_i(x_i)$.

The variance-based sensitivity indices (Var-SI) [4, 5, 6] of component function f_u is defined by the ratio

$$\mathcal{S}_u = \frac{\mathrm{Var}(f_u)}{V}. \tag{9}$$

In particular, we note that the first-order Var-SI for input x_i can be written as

$$\mathcal{S}_i = \frac{\mathrm{Var}_{x_i}(E(y|x_i))}{V}, \tag{10}$$

and the variance-based total sensitivity index (Var-TSI) $\mathcal{S}_{i,\mathbf{T}}$ is

$$\mathcal{S}_{i,\mathbf{T}} = \sum_{\substack{\emptyset \neq u \subseteq \{1,\ldots,N\} \\ i \in u}} \mathcal{S}_u = \frac{E(\mathrm{Var}_{x_i}(y|\vec{x}_{-i}))}{V}, \tag{11}$$

where $\vec{x}_{-i}$ indicates exclusion of input parameter x_i. From (8), all Var-SI are non-negative and sum to unity. Both $0 \leq \mathcal{S}_{i,\mathbf{T}} \leq 1$ and $\sum_{i=1}^{N} \mathcal{S}_{i,\mathbf{T}} \geq 1$ are guaranteed.

A more practical integral representation of $\mathcal{S}_{i,\mathbf{T}}$ in (11) has been proposed by Sobol' [5] to ease the Monte Carlo (MC) estimation of Var-TSI

$$\mathcal{S}_{i,\mathbf{T}} = \frac{1}{2V} \int_{\mathbb{R}} \int_{\mathbb{R}^N} \left[f(x_i', \vec{x}_{-i}) - f(\vec{x}) \right]^2 \mathrm{d}F(\vec{x})\, \mathrm{d}F_i(x_i'). \tag{12}$$

The importance of Var-TSI $\mathcal{S}_{i,\mathbf{T}}$ is in that the model approximation error—when fixing $x_i = x_i^0$—strongly depends on it. Sobol' et al. [7] defined the following model error

$$\delta(x_i^0) = \frac{1}{V} \int_{\mathbb{R}^N} \left[f(x_i^0, \vec{x}_{-i}) - f(\vec{x}) \right]^2 \mathrm{d}F(\vec{x}), \tag{13}$$

and showed that for an arbitrary x_i^0 the error $\delta(x_i^0) \geq \mathcal{S}_{i,\mathbf{T}}$. If we consider x_i^0 as random and following the distribution $F_{x_i}(x_i)$, by comparing (12) and (13) we immediately have the error's expectation

$$E(\delta(x_i^0)) = 2\mathcal{S}_{i,\mathbf{T}}. \tag{14}$$

According to (14), if uncertain input parameters that have small Var-TSI values are fixed to their nominal (or other) values, the model output uncertainty essentially remains the same in an L_2 metric sense. Therefore, Var-TSI are widely accepted as an importance ranking tool for dimensionality reduction.

It is, however, well-understood that costs can be high for estimating (12) by Monte Carlo approaches [8, 9, 10], because of the slow convergence rate of Monte Carlo methods and due to the need to establish independent realizations of the input parameter x_i'. Thus we consider a multivariate polynomial expansion of the ANOVA representation (5), and further explore the straightforward computation of global sensitivity indices by a post-processing of polynomial coefficients.

4 Multivariate Polynomial Surrogate Construction

The primary purpose here is to develop an efficient method to compute Var-TSI (11) or (12). While it is always possible to estimate these integrals by crude Monte Carlo to obtain realizations of computer simulations, this approach is prohibitive in many challenging cases due to computational cost. Using a reliable polynomial surrogate to replace the original simulation model can provide an efficient method, especially when the output statistics and sensitivity indices can be obtained from the coefficients of polynomial expansions.

4.1 Polynomial Dimensional Decomposition

A set of orthonormal univariate polynomials is defined as $\{\psi^j(x); j = 0, 1, \ldots\}$, where $\psi^j(x)$ has degree j and any two polynomials in the set are orthonormal, so

$$E(\psi^j(x)\psi^k(x)) = \begin{cases} 1 & j = k, \\ 0 & j \neq k. \end{cases} \tag{15}$$

For a vector $\vec{x}$ of N independent random variables, it should be clear that for any $\emptyset \neq u \subseteq \{1, \ldots, N\}$, and a positive multi-index $j_u = \{j_1, \ldots, j_{|u|}\} \in \mathbb{N}^{|u|}$,

$$\Psi_u^{j_u}(\vec{x}_u) = \prod_{k=1}^{|u|} \psi_{i_k}^{j_k}(x_{i_k})$$

is a multivariate orthonormal polynomial in $\vec{x}_u$ having degree $|j_u| = \sum_{k=1}^{|u|} j_k$. The following properties result:

$$E(\Psi_u^{j_u}(\vec{x}_u)) = 0,$$

and

$$E(\Psi_u^{j_u}(\vec{x}_u)\Psi_v^{j_v}(\vec{x}_v)) = \begin{cases} 1 & u = v, j_u = j_v, \\ 0 & \text{otherwise.} \end{cases}$$

The space of all real polynomials in $\vec{x}$, denoted by $\mathscr{P}^N$, admits the following orthogonal decomposition [11]

$$\mathscr{P}^N = \mathbf{1} \oplus \bigoplus_{\emptyset \neq u \subseteq \{1,\ldots,N\}} \text{span}\{\Psi_u^{j_u}(\vec{x}_u) : j_u \in \mathbb{N}^{|u|}\}, \tag{16}$$

with $\oplus$ representing the orthogonal sum. Thus, the polynomial dimensional decomposition (PDD) [12] for any random variable $f(\vec{x}) \in L^2(\mathbb{R})$ is a Fourier series in multivariate orthonormal polynomials in $\vec{x}$,

$$f(\vec{x}) = f_0 + \sum_{\emptyset \neq u \subseteq \{1,\ldots,N\}} \sum_{j_u} C_u^{j_u} \Psi_u^{j_u}(\vec{x}_u), \tag{17}$$

with $f_0 = E(f(\vec{x}))$. Comparing (17) with the ANOVA decomposition (5), the component function can be represented as

$$f_u(\vec{x}_u) = \sum_{j_u} C_u^{j_u} \Psi_u^{j_u}(\vec{x}_u).$$

We use (17) as our basic approach to represent high-dimensional input-output model response. Particularly, we use least-squares regression (LSR) to compute the coefficients $C_u^{j_u}$. However, it does not scale well with dimension. The next subsection presents an adaptive method to avoid this so-called curse of dimensionality using PDD.

4.2 Adaptive ANOVA and regression-based sparse PDD

The adaptive method adopted for PDD is based on the approach proposed by Tang et al. [13]. It has been successfully applied to turbulent combustion with complex and arbitrary input distributions to estimate variance- and covariance-based global sensitivity indices [14].

4.2.1 Truncation dimension

The low-order interactions of input variables are known to impact output [4, 15], and it might be argued that this is a characteristic of a well-designed physical model. This motivates truncation of the full ANOVA expansion (5) as

$$f(\vec{x})_\lambda = \sum_{\substack{u\subseteq\{1,\dots,N\}\\ |u|\leq\lambda}} f_u(\vec{x}_u), \text{ with } \lambda \ll N, \tag{18}$$

where λ is the truncation (or effective) dimension. This obvious first step reduces the size of the ANOVA expansion from (6) to

$$P_{\text{ANOVA},\lambda} = 1 + N + \binom{N}{2} + \cdots + \binom{N}{\lambda}, \tag{19}$$

which will typically be much smaller. For example, with $N = 50$ and $\lambda = 2$, $P_{\text{ANOVA},\lambda} \approx 10^{-12} \times P_{\text{ANOVA}}$.

4.2.2 Variance-based adaptive ANOVA — Active dimension

For problems with a high dimensionality, it is advantageous to further reduce the $P_{\text{ANOVA},\lambda}$ number in (19) to the following

$$P_{\text{ANOVA},(\lambda,D)} = 1 + N + \binom{D}{2} + \cdots + \binom{D}{\lambda}, \tag{20}$$

where $D \leq N$ is called an active dimension. Note that the first-order ANOVA components are retained in (20). This accounts for their potential significant contribution, and $\sim N$ is not deemed overly expensive.

Choosing the uncertain parameters $x_{i_1}, \dots, x_{i_D}$ that are included in second- and higher-order ANOVA components is then necessary. For this, we use the criterion proposed by Yang et al. [16]. Using a LSR approach, a first-order ANOVA-PDD expansion is constructed with the highest univariate polynomial degree equal to m,

$$f^{(1)}_{\text{PDD},m}(\vec{x}) = f_0 + \sum_{i=1}^{N} \left(\sum_{j=1}^{m} C_i^j \psi^j(x_i) \right). \tag{21}$$

The Sobol' global sensitivity index is then estimated by

$$\mathcal{S}_i = \frac{\sum_{j=1}^{m} (C_i^j)^2}{\sum_{k=1}^{N} \sum_{j=1}^{m} (C_k^j)^2}. \tag{22}$$

Assuming a monotonically decreasing $\mathcal{S}_{i_k}, k = 1, \ldots, N$, we choose D to satisfy

$$\sum_{k=1}^{D} \mathcal{S}_{i_k} \geq p. \tag{23}$$

As crafted, the threshold p in (23) is a constant close to the unity (e.g., $p = 0.99$). The rationale of using (23) is in that we exclude—for second- and higher-order ANOVA components—all parameters whose total variance contribution is small (less than 1 % for $p = 0.99$) in a first-order ANOVA expansion.

4.2.3 Adaptive least-squares regression

To keep the model size small (i.e., the system sparse), we augment the existing polynomial set (21) by recursively adding new polynomial candidates one-at-a-time from the set of higher-order ANOVA functions. During this recursive procedure, we eliminate polynomials that are quantified as *unimportant*. To measure this relative importance we use a variance-based criterion. For this procedure, a stepwise regression technique is used, which eliminates polynomial $\Psi_v^{j_v}(\vec{x}_v)$ satisfying

$$\frac{(C_v^{j_v})^2}{\sum\limits_{\emptyset \neq u \subseteq \{1,\ldots,N\}} \sum\limits_{j_u} (C_u^{j_u})^2} < \theta, \tag{24}$$

where θ is a pre-selected threshold, which can be adjusted to accelerate convergence for the particular application. Thus, these nominally unimportant polynomials are eliminated following each LSR during the recursive procedure. The size of a regression is restricted in a controlled way, so that the ANOVA polynomial surrogate is sufficiently sparse during this adaptive step, and the needed number of model evaluations remains sufficiently small.

4.2.4 Global sensitivity indices based on polynomial coefficients

Once the polynomial expansion has been finally determined following the recusive and adaptive approach described previously, the output statistics and sensitivity indices can be readily obtained. The mean of QoI is the constant term of the expansion

$$E(f) = f_0, \tag{25}$$

and the total output variance is the sum of squares of coefficients of all non-constant polynomial terms

$$V(f) = \sum_{\emptyset \neq u \subseteq \{1,\ldots,N\}} \sum_{j_u} (C_u^{j_u})^2. \tag{26}$$

Var-SI of component function f_u is then computed as

$$\mathcal{S}_u = \sum_{j_u} (C_u^{j_u})^2 \Big/ V(f), \tag{27}$$

and the total sensitivity (Var-TSI, $\mathcal{S}_{i,\mathbf{T}}$) of parameter x_i is obtained by simply adding all $\{\mathcal{S}_u | i \in u\}$.

5 Results for materials with isotropic components

Parsl [17] has been used in this work to conveniently schedule and allocate computational resources for Monte Carlo sample runs. Parallelism across sample runs were easily managed with the aim of maximizing the use of nodes/cores. In this section, we first realize a convergence study in terms of grid resolution in PuMA, and then construct an adaptive ANOVA based polynomial surrogate which provides knowledge on relative importances of uncertain parameters.

5.1 Resolution study

In PuMA, a domain size (n_1, n_2, n_3 in the three main orthogonal directions) is required to computationally generate a representative elementary volume (REV) [2], which is the size at which a sample of the microstructure is representative of the macroscale material structure. In this paper, we consider a cube whose physical length is fixed to be equal to the nominal fiber length, i.e., $d_1 = d_2 = d_3 = 1\,\text{mm}$. For simplicity, we take equal resolution size at all directions $n_1 = n_2 = n_3 = n$. Thus, the voxel length of $1/n\,\text{mm}$ is assigned to the material.

The fast explicit jump solver harmonic averaging method used in this paper was developed by Wiegmann and Zemitis [3] to estimate the effective thermal conductivity of composite materials. This method is known to have first-order convergence with respect to voxel resolution. We investigate here the convergence of the effective conductivity, which allows us to know the minimum n required to compute accurate material properties. Figure 2 illustrates the effective conductivities in three orthogonal directions in function of voxel size. It shows we have very accurate estimation starting from a discretization with approximately 500^3 points.

5.2 Polynomial-based surrogate and sensitivity analysis

The purpose of this section is to construct a polynomial-based surrogate with the benefit of ranking parameter importances thanks to the Sobol's total indices that are easily derived from the mathematical representation of the surrogate (see Sections 3 and 4). We also show how these sensitivity indices change with increasing domain sizes.

Because of the typical high cost of UQ sampling, it is natural to start with a rather low resolution (100^3) for the PuMA solver. Figure 3a and Figure 3b show 200 sampling data of $k_{\text{eff},1}$ (labeled as "QoI 1") with respect to the porosity ϕ and the fiber diameter variation Δd_{fiber}, which show a qualitative strong and weak dependency, respectively. A histogram pdf is shown in Figure 3c. The sample number 200 retained in this study is not chosen entirely randomly. Following our experience reported [13, 14, 18], 200 is in most cases sufficient to construct a very accurate PDD surrogate for a 10-dimensional problem (as will be demonstrated later), thanks to the outstanding performance of our multi-level adaptive approach described in Section 4. Our choice of such a low sample size also aligns well with the overall UQ goal of lowering the computational cost without compromising accuracy.

An advantage of using the approach described in Section 4 is that a global sensitivity analysis and a polynomial-based surrogate are simultaneously available for a very low cost, in terms of the number of simulation runs required for the thermal conductivity computation. With only 200 training points generated by a conventional MC approach, Figure 4 shows the approximation accuracy of our polynomial-based surrogate. With an

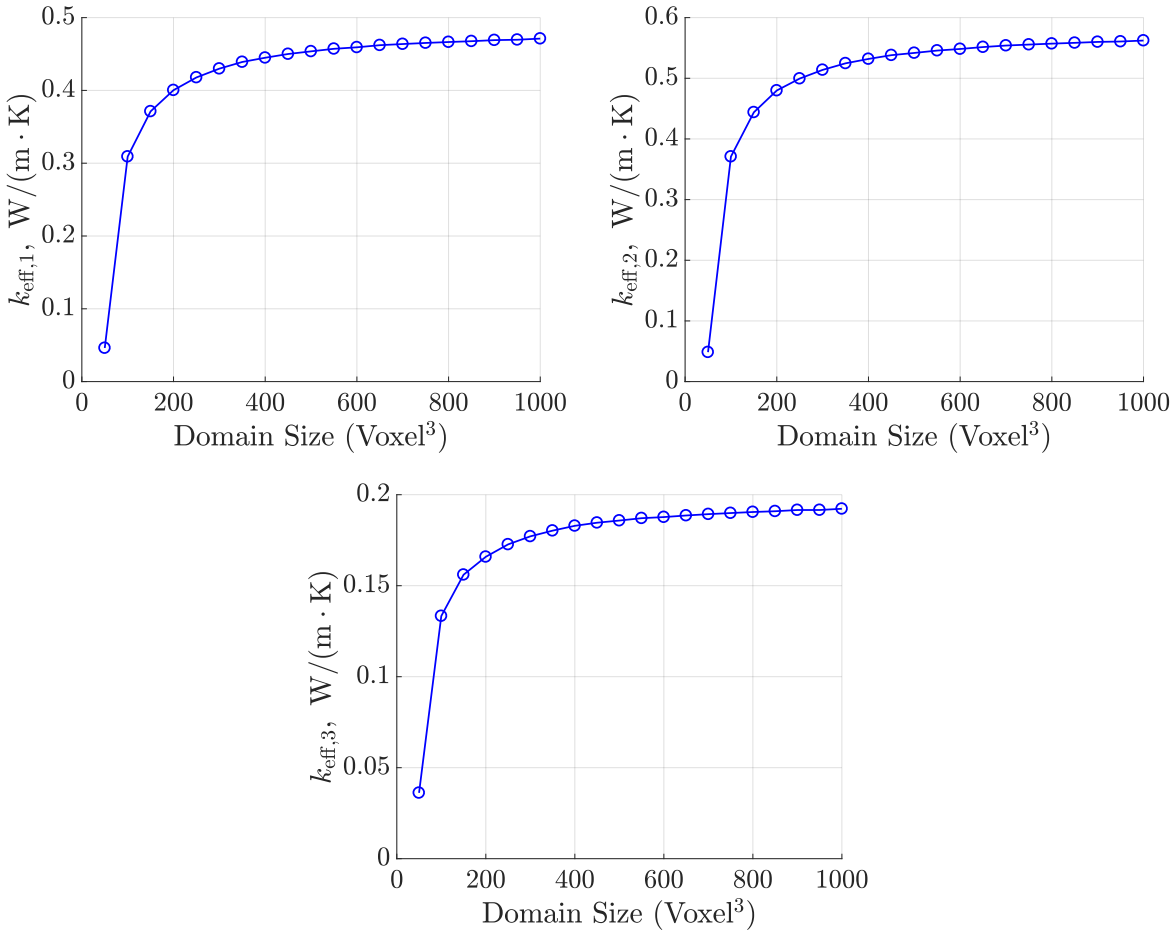

Figure 2: Computed effective thermal conductivity of artificially generated cylinder fibers versus domain size (voxel^3).

increasing domain size from 100^3 until 512^3, both the standard and leave-one-out cross-validation based accuracy estimates (R^2 and Q^2, respectively; readers are refereed to Tang et al. [13, 14] for the rigorous definitions of these estimates) are very close to unity, indicating a sufficiently accurate approximation.

Figure 5a illustrates a ranking of importances for the 10 parameters considered. The measure used is the standard Sobol' total sensitivity indices. Results are shown for domain sizes between 100 and 512. We observe that the ranking is consistant between low and high domain sizes. This is beneficial since one can further realize sensitivity analyses by increasing the number of sample runs and retaining a rather low domain size of the physical problem.

Figure 5b shows the total variance of $k_{\text{eff},1}$ divided by its contributers. This further confirms that the Var-TSI are accurate even though the total variance is rather not converged yet. This is encouraging as part of our multi-fidelity strategy which aims to obtain the most accurate results with limited computational resources.

6 Conclusions

This paper has sought to investigate the impact of model parameters and their uncertainties on the effective thermal conductivity of locally isotropic (and globally anisotropic) microstructures, which are artificially generated using the PuMA software [2]. Among all

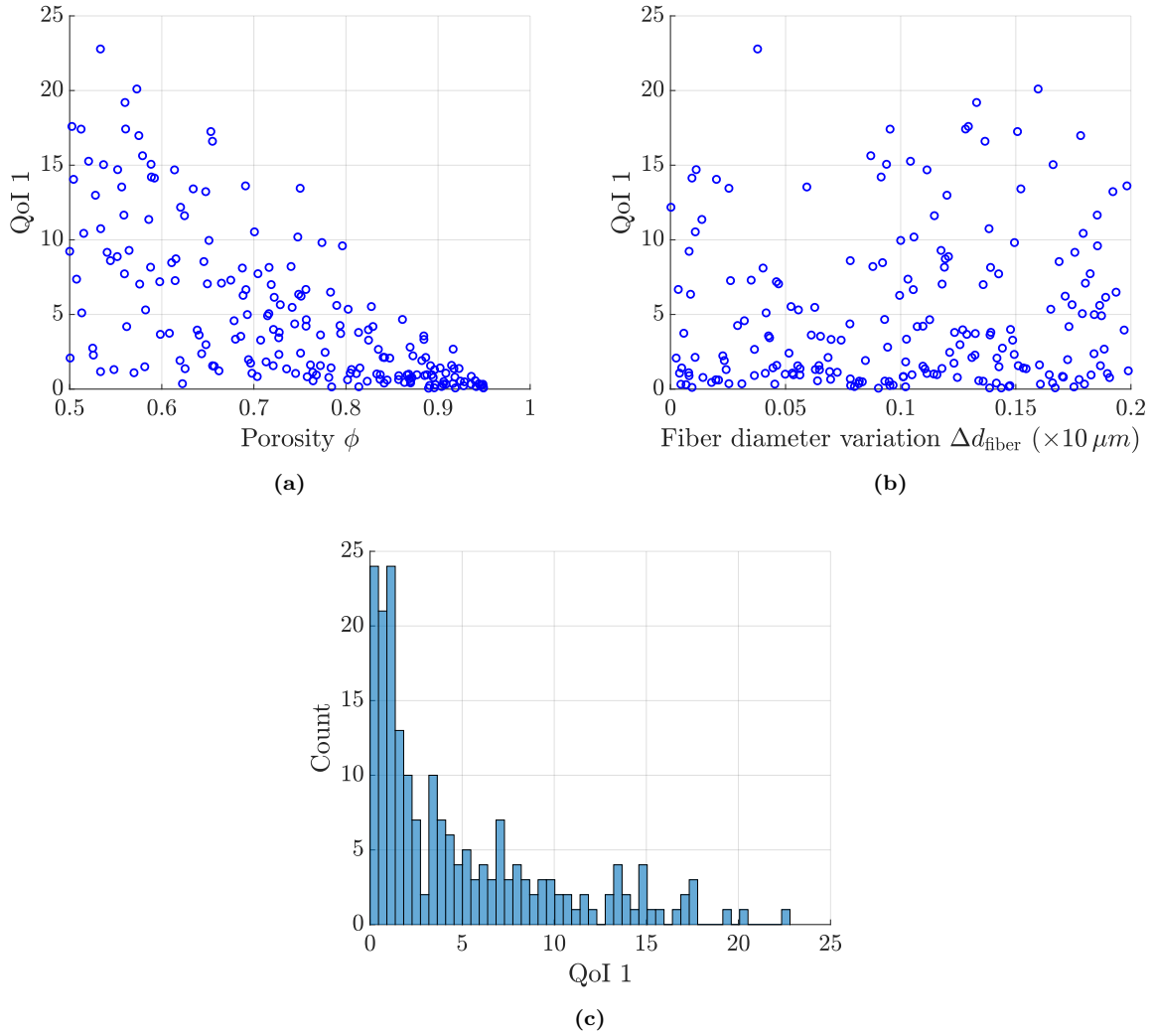

Figure 3: The qualitative impact of an important parameter (porosity (a)) versus an unimportant one (fiber diameter variation (b)) over the output $k_{\text{eff},1}$ (labeled as "QoI 1"), with the output distribution shown (c).

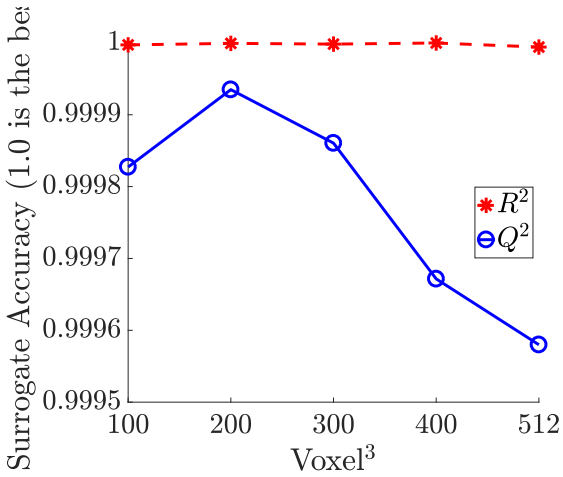

Figure 4: Polynomial approximation accuracy with respect to the domain sizes.

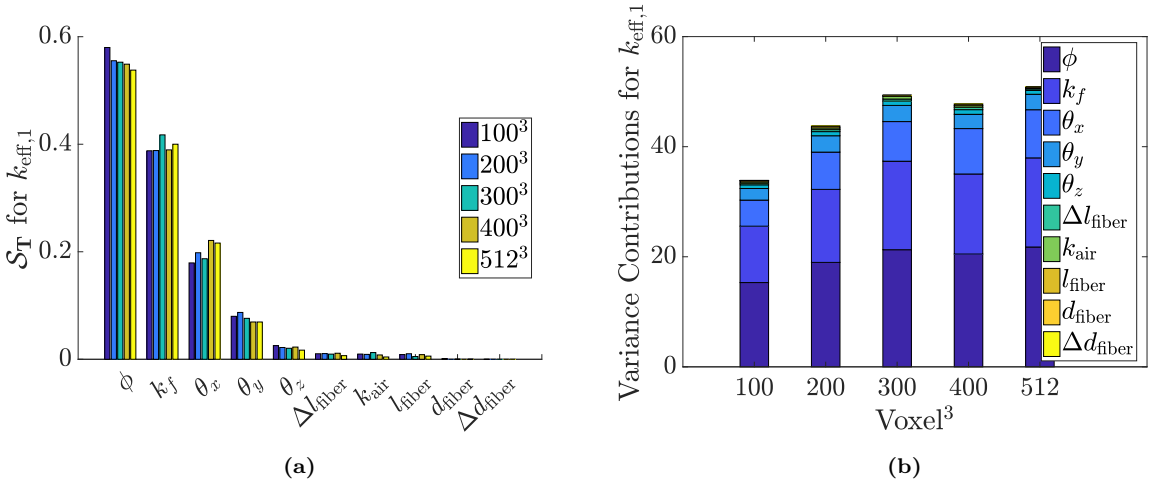

Figure 5: Total sensitivity indices (a) and variance contributions (b) of input parameters, computed using various domain sizes.

considered uncertain parameters, it has been found that the porosity has the most significant contribution to the uncertainty of a material's effective thermal property. Furthermore, it has been found the importance ranking among parameters is insensitive to the mesh size of the heat transfer problem. Our future work will be focused on microstructures with locally anisotropic components, whose analysis is more challenging because of the significantly higher computational cost [19].

Acknowledgment

This material is based in part upon work supported by the Department of Energy, National Nuclear Security Administration, under Award Number DE-NA0003963.

References

[1] Andy Vanaerschot, Francesco Panerai, Alan Cassell, Stepan V. Lomov, Dirk Vandepitte, and Nagi N. Mansour. Stochastic characterisation methodology for 3-d textiles based on micro-tomography. *Composite Structures*, 173:44 – 52, 2017. ISSN 0263-8223. doi: https://doi.org/10.1016/j.compstruct.2017.03.107. URL `http://www.sciencedirect.com/science/article/pii/S0263822316323340`.

[2] Joseph C. Ferguson, Francesco Panerai, Arnaud Borner, and Nagi N. Mansour. Puma: the porous microstructure analysis software. *SoftwareX*, 7:81 – 87, 2018. ISSN 2352-7110. doi: https://doi.org/10.1016/j.softx.2018.03.001. URL `http://www.sciencedirect.com/science/article/pii/S2352711018300281`.

[3] A. Wiegmann and A. Zemitis. Ej-heat: A fast explicit jump harmonic averaging solver for the effective heat conductivity of composite materials. Technical Report 94, Fraunhofer (ITWM), 2006. URL `http://nbn-resolving.de/urn:nbn:de:hbz:386-kluedo-17860`.

[4] I. M. Sobol'. Sensitivity estimates for nonlinear mathematical models. *Mathematical Modelling & Computational Experiments*, 1(4):407–414, 1993.

[5] I. M. Sobol'. Global sensitivity indices for nonlinear mathematical models and their

Monte Carlo estimates. *Mathematics and Computers in Simulation*, 55(1-3):271–280, feb 2001. ISSN 03784754. doi: 10.1016/S0378-4754(00)00270-6. URL http://linkinghub.elsevier.com/retrieve/pii/S0378475400002706.

[6] Andrea Saltelli. Making best use of model evaluations to compute sensitivity indices. *Computer Physics Communications*, 145(2):280–297, 2002. ISSN 00104655. doi: 10.1016/S0010-4655(02)00280-1.

[7] I.M. Sobol', S. Tarantola, D. Gatelli, S.S. Kucherenko, and W. Mauntz. Estimating the approximation error when fixing unessential factors in global sensitivity analysis. *Reliability Engineering & System Safety*, 92(7):957–960, jul 2007. ISSN 09518320. doi: 10.1016/j.ress.2006.07.001. URL http://linkinghub.elsevier.com/retrieve/pii/S0951832006001499.

[8] S. Kucherenko, M. Rodriguez-Fernandez, C. Pantelides, and N. Shah. Monte Carlo evaluation of derivative-based global sensitivity measures. *Reliability Engineering and System Safety*, 94(7):1135–1148, 2009. ISSN 09518320. doi: 10.1016/j.ress.2008.05.006.

[9] I.M. Sobol' and S. Kucherenko. Derivative based global sensitivity measures and their link with global sensitivity indices. *Mathematics and Computers in Simulation*, 79(10):3009–3017, 2009.

[10] I.M. Sobol' and S. Kucherenko. A new derivative based importance criterion for groups of variables and its link with the global sensitivity indices. *Computer Physics Communications*, 181(7):1212–1217, 2010.

[11] Sharif Rahman. Mathematical properties of polynomial dimensional decomposition. *SIAM/ASA Journal on Uncertainty Quantification*, 6(2):816–844, jan 2018. ISSN 2166-2525. doi: 10.1137/16M1109382. URL https://epubs.siam.org/doi/10.1137/16M1109382.

[12] Sharif Rahman. A polynomial dimensional decomposition for stochastic computing. *International Journal for Numerical Methods in Engineering*, 76:2091–2116, 2008. doi: 10.1002/nme. URL http://onlinelibrary.wiley.com/doi/10.1002/nme.2394/abstract.

[13] Kunkun Tang, Pietro M. Congedo, and Rémi Abgrall. Adaptive surrogate modeling by ANOVA and sparse polynomial dimensional decomposition for global sensitivity analysis in fluid simulation. *Journal of Computational Physics*, 314:557–589, 2016. ISSN 00219991. doi: 10.1016/j.jcp.2016.03.026. URL http://linkinghub.elsevier.com/retrieve/pii/S0021999116001789.

[14] Kunkun Tang, Luca Massa, Jonathan Wang, and Jonathan B. Freund. An adaptive least-squares global sensitivity method and application to a plasma-coupled combustion prediction with parametric correlation. *Journal of Computational Physics*, 361:167–198, 2018. ISSN 00219991. doi: 10.1016/j.jcp.2018.01.042. URL http://linkinghub.elsevier.com/retrieve/pii/S0021999118300524.

[15] Herschel Rabitz, Ömer F. Alis, Jeffrey Shorter, and Kyurhee Shim. Efficient input-output model representations. *Computer Physics Communications*, 117(1-2):11–20, 1999.

[16] X. Yang, M. Choi, G. Lin, and G. E. Karniadakis. Adaptive ANOVA decomposition of stochastic incompressible and compressible flows. *Journal of Computational Physics*, 231(4):1587–1614, feb 2012. ISSN 00219991. doi: 10.1016/j.jcp.2011.10.028. URL http://dx.doi.org/10.1016/j.jcp.2011.10.028.

[17] Yadu Babuji, Anna Woodard, Zhuozhao Li, Daniel S. Katz, Ben Clifford, Rohan Kumar, Lukasz Lacinski, Ryan Chard, Justin M. Wozniak, Ian Foster, Michael Wilde, and Kyle Chard. Parsl: Pervasive parallel programming in python. In *Proceedings of the 28th International Symposium on High-Performance Parallel and Distributed Computing*, HPDC '19, pages 25–36, New York, NY, USA, 2019. Association for Computing Machinery. ISBN 9781450366700. doi: 10.1145/3307681.3325400. URL https://doi.org/10.1145/3307681.3325400.

[18] Kunkun Tang, Jonathan M. Wang, and Jonathan B. Freund. Adaptive sparse polynomial dimensional decomposition for derivative-based sensitivity. *Journal of Computational Physics*, 391:303–321, 2019. ISSN 0021-9991. doi: https://doi.org/10.1016/j.jcp.2019.04.042. URL https://www.sciencedirect.com/science/article/pii/S0021999119302888.

[19] Federico Semeraro, Joseph C. Ferguson, Marcos Acin, Francesco Panerai, and Nagi N. Mansour. Anisotropic analysis of fibrous and woven materials part 2: Computation of effective conductivity. *Computational Materials Science*, 186:109956, 2021. ISSN 0927-0256. doi: https://doi.org/10.1016/j.commatsci.2020.109956. URL https://www.sciencedirect.com/science/article/pii/S092702562030447X.